

Interactive comment on “Characteristics of earthquake ruptures and dynamic off-fault deformation on propagating faults” by Simon Preuss et al.

Simon Preuss et al.

simon.preuss@erdw.ethz.ch

Received and published: 16 June 2020

Dear Editor,

Thank you for your helpful comments on our manuscript entitled “Characteristics of earthquake ruptures and dynamic off-fault deformation on propagating faults” [Paper se-2020-16]. We are grateful for the constructive and thoughtful comments made by the reviewers. We have addressed their questions, which are quoted below in blue. Text in red indicates text added to the new version of the manuscript. We also provide a PDF version of the revised manuscript in which we highlighted the changes in red (deleted) and blue (added). All line numbers in the letter below refer to the tracked-

C1

changes document. We hope that our revised manuscript has clarified the questions raised by the reviewers and made the paper stronger.

Best regards, Simon Preuss (on behalf of all co-authors)

Reviewer 2 - Boris Kaus 1.1) Yield stress criteria You correctly write that at yield $F=0$, and you employ a standard Drucker-Prager yield function (eq. 9). Yet, your expression for the yield function (eq. 8) is incorrect, which can be best illustrated graphically:

The plot shows the yield function (black) together with the Mohr-Circle (green circle, which has radius $\delta\sigma_{II}^0$). At yielding ($F=0$), the Mohr-Circle exactly touches the yield stress function. This condition is not $\delta\sigma_{II}^0 = \delta\sigma_{II}^0 \tan(\delta\theta)$ (your eq. 4), as this gives the red circle (which predicts a stress that is somewhat larger than the yield stress). Instead, we can use trigonometry to compute the condition for $F=0$. If we define the effective angle of friction $\delta\theta$ as: $\tan \delta\theta = \frac{\delta\sigma_{II}^0}{\delta\sigma_{I}^0} (1 - \delta\lambda)$, we can define the yield condition ($F=0$) as: $\delta\sigma_{II}^0 = \delta\sigma_{I}^0 \sin(\delta\theta) + \delta\sigma_{III}^0 \cos(\delta\theta)$

Since this is correctly described in the textbook of one of the co-authors of this manuscript, I suspect that it is incorporated correctly in the software. I also don't know how big an effect it will make on the results, even if this would not be the case (to be tested). Yet, in any case, it would be good if you can correct your description.

We thank the reviewer for this important comment and a clarifying discussion, which together helped improving the paper. We clarified the yielding function description and changed notations to avoid confusion. We use a modified Drucker-Prager yielding condition with constant compressive strength and variable friction coefficient. We changed the method description in line 141: The onset of plastic deformation is defined by the yield criterion:

$$F = \tau_{II} - \sigma_C - \mu_{\text{eff}}(\text{RSF}) P_{\text{eff}},$$

where $P_{\text{eff}} = P - P_{\text{fluid}} = P (1 - \lambda)$ with the pore fluid pressure factor $\lambda = P_{\text{fluid}}/P$

C2

, σ_c is the constant compressive strength that marks the residual strength at $P = 0$ and $\mu_{\text{eff}}(\text{RSF})$ is a variable effective friction parameter that we define based on our continuum RSF formulation. We use a modified Drucker-Prager plastic yield function (Drucker and Prager, 1952) in the form: $\sigma_{\text{yield}} = C(\text{RSF}) + \mu(\text{RSF}) P_{\text{eff}}$ where

$\mu(\text{RSF}) = \tan(\sin^{-1}(\mu_{\text{eff}}(\text{RSF})))$ is the local friction coefficient that is widely used and obtained from laboratory experiments and

$C(\text{RSF}) = \sigma_c / \cos(\sin^{-1}(\mu_{\text{eff}}(\text{RSF})))$ is the local cohesion.

The local effective friction parameter $\mu_{\text{eff}}(\text{RSF})$ evolves according to the invariant reformulation of rate- and state-dependent friction for a continuum, introduced by Herdörfer et al. (2018). This formalism was applied to freely and spontaneously growing seismic and aseismic faults by Preuss et al. (2019), by interpreting how plastic deformation starts to localize and forms a shear band that approximates a fault zone of finite width that can host earthquakes. Localized bulk deformation and fault slip are related by defining the plastic slip rate V_p as

$$V_p = 2\varepsilon \dot{\gamma} W, \quad \dot{\gamma} = \frac{1}{L} \frac{d\theta}{dt}$$

where W denotes the width of the fault zone in the continuous host rock. We formulate $\mu_{\text{eff}}(\text{RSF})$ as:

$$\mu_{\text{eff}}(\text{RSF}) = a \operatorname{arcsinh} \left(\frac{V_p / 2V_0 \exp((\mu_0 + C/P + b \ln(\theta V_0/L))/a)}{1} \right),$$

where a and b are laboratory-based, empirical RSF parameters that quantify a direct effect and an evolution effect of friction, respectively, L is the RSF characteristic slip distance, μ_0 is a reference friction coefficient at a reference slip velocity V_0 (Lapusta and Barbot, 2012), and C is the cohesion as part of the state variable θ (Marone et al., 1992) that evolves according to the aging law:

$$d\theta/dt = 1 - V_p \theta / L.$$

Additionally, we updated Figure 4 according to the recomputed relative fault angles

C3

based on equation 9.

1.2) Elastic material parameters Your choice of having the same values for bulk and shear moduli (table 1; both 50 GPa) results in a Poisson ratio of 0.125. That might be appropriate for already damaged rocks, but perhaps not so much for intact rocks. How sensitive are your results to the particular choice of Poisson ratio? We thank the reviewer for this question. A Poisson's ratio of 0.125 is on the lower end of values for rocks, but still common for a wide range of rocks as for example shown in Poisson's ratio values for rocks (H. Gercek, 2007). Furthermore, we tested a range of shear moduli resulting in varying Poisson's ratios and found only a marginal impact on the model results. In particular, the main messages of our manuscript are not influenced by changes in the Poisson's ratio. We illustrate this by comparing the snapshots of simulations with Poisson's ratio of 0.125 and 0.25. We focus on the dynamically generated off-fault yielding at approximately the same deformation stage just before the rupture hits the end of the predefined fault. Both snapshots are attached. The differences comprise: \bullet First earthquake nucleates 75 years later for $\nu = 0.25$. \bullet The maximum slip velocity is ~ 0.08 m/s higher for $\nu = 0.25$. \bullet The off-fault splay localization is more irregular with a higher degree of localization and a slightly higher off-fault reach for $\nu = 0.25$.

Fig.1 Fig.2

In light of our answer above we add to line 703 of the manuscript: Our choice of parameters results in a Poisson ratio of 0.125. Such a relatively low Poisson's ratio is on the lower end of values for rocks, but still common for a wide range of rock types as for example shown in Gercek (2007). To illustrate the impact of different Poisson's ratios we have tested a range of different shear moduli resulting in varying Poisson's ratios. These tests have shown that the main messages of our manuscript are not influenced by changes in the Poisson's ratio.

2) Minor remarks: \bullet Table 1: I suppose that the host rock cohesion is 6 MPa, and

C4

not 6e6 MPa? This is correct. We changed that. \hat{U} Fig. 3: you show an overview of several different models. Yet, are the snapshots chosen to have approximately the same plastic strain, deformation stage or \hat{A} time? Would be good to mention it. Thanks for this comment. We added the following to the figure caption: The snapshots in [a] are chosen to have approximately the same deformation stage with regard to fault length 'R*1'. Model RW constitutes an exception as RW1 remains very short (1.8 km, see main text). \hat{U} Figure 4. It would be good to explain at the beginning of the figure caption that \hat{A} this figure concerns the RT model. We agree and added a short note. \hat{U} Your movies are extremely large (some over 1 Gb!); it is certainly possible to create smaller movie-sizes from a set of pictures, and I believe that this is important for readers that do not have a high bandwidth connection. We agree. All movies are now approx. 5 times smaller with a maximum size of 122 Mb. These smaller videos can be uploaded upon resubmission.

Please also note the supplement to this comment:

<https://se.copernicus.org/preprints/se-2020-16/se-2020-16-AC2-supplement.pdf>

Interactive comment on Solid Earth Discuss., <https://doi.org/10.5194/se-2020-16>, 2020.

C5

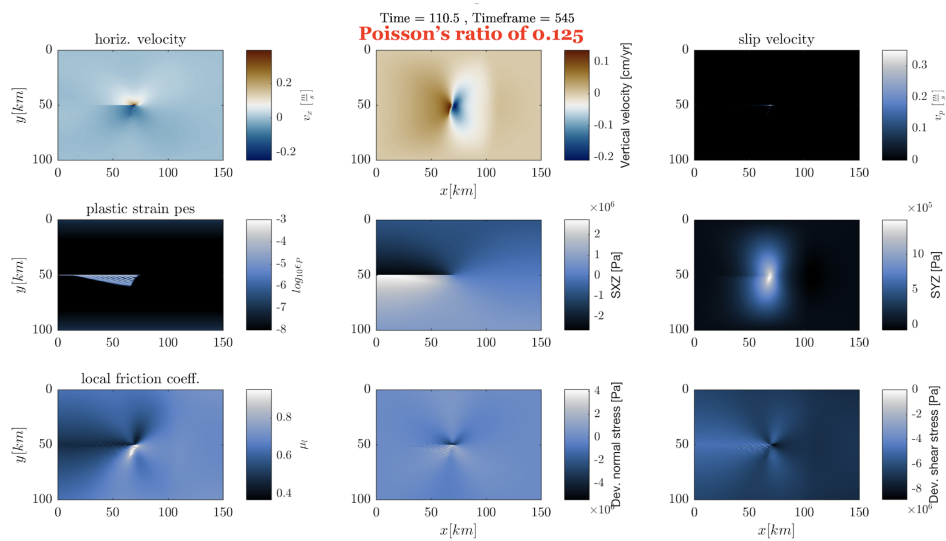


Fig. 1.1.2_Fig1

C6

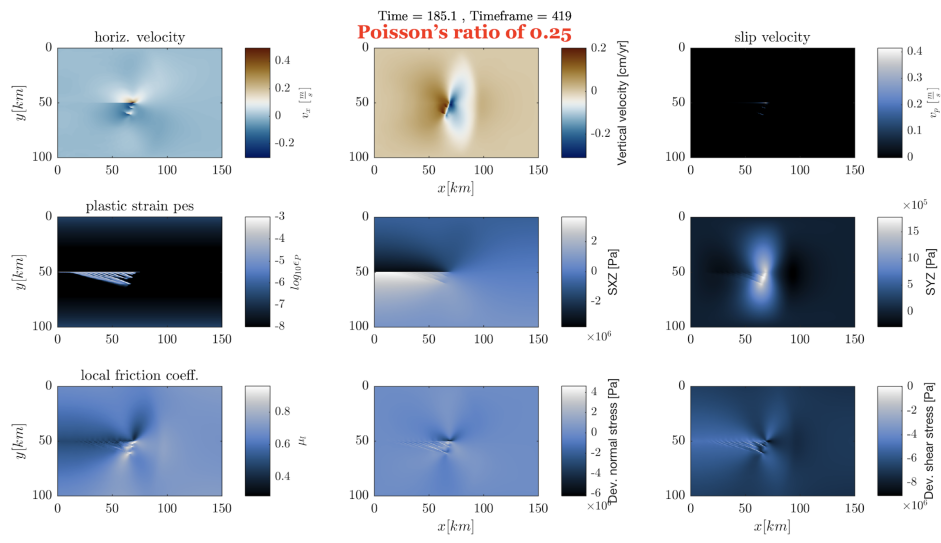


Fig. 2. 1.2_Fig2